Novel synthesis route to graphene using iron nanoparticles

Rajen B. Patel[a] and Chi Yu
Department of Materials Science and Engineering, New Jersey Institute of Technology, Newark, New Jersey 07102, USA

Tsengming Chou
Department of Chemical Engineering and Materials Science, Laboratory for Multiscale Imaging, Stevens Institute of Technology, Hoboken, New Jersey 07030, USA

Zafar Iqbal
Department of Chemistry and Environmental Science, New Jersey Institute of Technology, Newark, New Jersey 07102, USA

(Received 2 January 2014; accepted 20 June 2014)

Graphene is currently one of the most extensively studied materials because it displays a number of unique structural and electronic properties. A variety of methods are currently available for the growth of graphene; however, few are viable for large scale, cost-effective production of high quality graphene. Here, a novel growth process for few layer graphene using chemical vapor deposition (CVD) and a commercial iron nanopowder catalyst is described. This method is readily scalable so it can be used to produce a large volume of graphene sheets. Graphene sheets made from this process were characterized by Raman spectroscopy, and scanning and transmission electron microscopy. Raman spectroscopy shows that the product consists of few layer graphene sheets. This is the first reported method of utilizing nanoparticles to synthesize graphene by a CVD process, which typically produces multiwalled carbon nanotubes. A possible mechanism for the formation of graphene by this modified CVD process is discussed.

I. INTRODUCTION

Graphene has attracted significant worldwide interest since the optimization in 2003 of the mechanical exfoliation approach, in particular, to produce high quality samples.[1,2] Graphene possesses a number of remarkable properties, for example: it has extremely high mechanical strength, it conducts electricity via ballistic fermions, displays chiral quantum effects, and is a single layer zero band gap semiconductor.[3] Graphene, therefore, has the potential to find use in a number of small and large scale applications. However, a significant challenge in the commercialization of graphene is that the material cannot yet be produced by a scalable process. Mechanical exfoliation, reduction of graphite oxide layers, and epitaxial growth on SiC wafers are all techniques which can produce high quality graphene, but these methods cannot be scaled up for bulk applications of this material. Chemical vapor deposition (CVD) processes can also form graphene, usually using copper or nickel substrates.[3] However, CVD methods prohibit economically viable manufacturing of bulk graphene because they must typically use a foil or thin film as a growth substrate. If graphene can be synthesized utilizing commercially available catalyst particles, the cost of graphene could approach that of multiwalled carbon nanotubes. Nickel particles were previously utilized as a catalyst to grow graphene, but the process used micrometer (generally <30 μm)-sized particles. This resulted in large area graphene sheets, but overall yields were low.[4] Copper and nickel are typically the catalytic metals of choice to grow graphene,[5–8] although iron has been widely used as a catalyst for the growth of related carbon nanostructures such as carbon nanotubes, and iron films have been shown to grow graphene.[9,10] If iron is used both as a matrix and catalyst to form metal–graphene nanocomposites, a number of structural applications become possible. This is because iron and steel have great intrinsic mechanical strength, especially when they have a particle size in the nanoscale regime.[11] Iron also easily connects carbon structures that could form hierarchical architectures and arrays.[12–15] However, since carbon is more soluble in iron than in copper, single layer graphene may be more difficult to grow on iron, but strong iron–carbon bonds would lead to high strength metal–graphene nanocomposites.

The CVD growth of graphene on spherical nanoparticles of transition metals would be unlikely to occur because this would typically result in the formation of amorphous carbon or carbon nanotubes.[12–16] Theoretically, there are two possible pathways for the formation of graphene on spherical nanoparticles. One is a 'flower'-based model, and the other is a 'wall'-based model. The flower-based model would involve layers of carbon encircling the iron catalyst particles, and once a critical

[a]Address all correspondence to this author.
e-mail: RajenBP@gmail.com
DOI: 10.1557/jmr.2014.165

 © Materials Research Society 2014

https://doi.org/10.1557/jmr.2014.165 Published online by Cambridge University Press

TABLE I. CVD parameters for different graphene samples synthesized.

Sample notation	Average particle diameter of Fe catalyst	Heating rate/min to 800 °C	Argon (300 sccm)	Acetylene (6 sccm)	Carbon monoxide (100 sccm)
A	20 nm	10 °C	Yes	Yes	Yes
B	100 nm	10 °C	Yes	Yes	Yes
C	20 nm	33 °C	No	Yes	Yes
D	20 nm	33 °C	Yes	No	Yes
E	20 nm	33 °C	Yes	Yes	No
F	20 nm	33 °C	Yes	Yes	Yes
G	Sample F purified with 6 M nitric acid				
H	20 nm	33 °C (to 800 °C and 985 °C)	Yes	(Methane, 6 sccm)	Yes

point in the deposition is reached, they would fold out as in a flower, where the petals are the graphene sheets. A wall-based model would have the graphene layers growing vertically on top of an iron particle to form 'fins'. The wall-based model would lead to graphene with dimensions limited by the circumference of the nanoparticles, while the flower-based model would provide graphene limited in size by the surface area of the particles. The work to be discussed describes the growth of graphene on commercial nanoscale iron particles. Raman spectroscopy, in combination with scanning and transmission electron microscopy (TEM), is used to characterize the graphene produced and determine the likely model of growth on the spherical particles.

II. EXPERIMENTAL

The details of the experiments conducted are included in the supplemental materials. To summarize, 20 nm and 100 nm iron particles purchased from American Elements (Boston, MA) were exposed to temperatures of 800 °C at atmospheric pressure and a variety of carbon containing and inert gases in different combinations. Experiments varying the heating rate were also conducted. The products of these reactions were examined with Raman spectroscopy using 632.8 nm laser excitation, together with scanning electron microscopy (SEM), and TEM on selected samples. The most promising material from the different batches was purified using dilute nitric acid to remove the iron catalyst. The experimental parameters used for the CVD processes are given in Table I. Additionally, an attempt to synthesize an iron–graphene composite in situ was also performed in the same way as high strength iron–carbon nanotube composites were prepared,[12–16] though no increase in strength was observed.

III. RESULTS AND DISCUSSION

The Raman spectra of graphene and graphite are well established.[17–23] In the case of single layer graphene, the most prominent features with 514.5 nm excitation consist of the fundamental G line at 1582/cm, the G′ line near 2700/cm (it is also referred to as 2D because it is the first overtone of the D line), and the disorder D line near 1350/cm, which arises from the breathing mode of six carbon-atom ring defects.[17,18] The 632.8 nm excitation used here causes the G′ line and D line, which are both strongly dispersive, to shift down to 2660/cm from 2700/cm and to 1330/cm from 1350/cm with 514.5 nm excitation, respectively. The dispersive behavior of the D and G′ lines stems from a double-resonance Raman process. The D line is activated by defects, whereas the G′ line does not require defect activation and has high resonant peak intensity exceeding that of the G line in single layer graphene.

https://doi.org/10.1557/jmr.2014.165 Published online by Cambridge University Press

A plot of the ratio of the integrated intensities of the G and G′ lines versus the number of graphene layers is given by Graf et al.[19] Single layer graphene has a single G′ line, and, as the number of layers increases up to 5, interlayer interactions lead to broadening as a result of splittings and upshift in frequency of the G′ line. Beyond 5 layers, the G′ line spectrum of graphene is the same as that of bulk graphite.

Raman and SEM analyses were performed to initially investigate which growth conditions provided the most promising samples under the different CVD parameters given in Table I. Figure 1(a) shows that sample A, prepared using 20 nm Fe particles, has a relatively high intensity D line at 1338/cm activated by defects, and a sharp single G′ line at 2661/cm, which is of greater intensity than the G line at 1582/cm. The approximate integrated intensity ratio of 0.43 for the G and G′ lines corresponds to about 2–3 layer graphene. The SEM image in Fig. 1(b) shows graphene sheets (arrowed) mixed with carbon covered catalyst particles. A small fraction of carbon nanotubes does form and is evident in the SEM image in Fig. 1(b).

Sample B, prepared using a 100 nm catalyst, has a Raman spectrum similar to that of sample A, indicating that few layer graphene is present in the sample (Fig. 2). A broad scattering feature peaking at the position of a relatively sharp single G′ line is evident. This suggests the presence of a higher degree of disorder associated with graphene in this sample, although the intensity of the defect-activated D line is the same as in sample A. Figure 2(b), which shows a lower spatial resolution SEM image of sample B, indicates that a larger fraction of carbon nanotubes are formed compared with sample A. This is probably due to the larger catalyst size used in its synthesis. This suggests that smaller catalyst particle sizes would be needed for the more efficient growth of single layer graphene.

Samples C to F were prepared with the 20 nm catalyst using a faster heating rate of 33 °C/minute relative to the 10 °C/minute rates for samples A and B. Faster heating rates were expected to prevent the growth of the catalyst particles during the CVD process. Sample C was prepared without using argon as a carrier gas; samples D and E were the only ones prepared without acetylene and CO, respectively, in the carrier gas. The Raman spectrum of sample F is displayed in Fig. 3, whereas those for samples C, D, E, and H are in Fig. S2. (All S labeled figures are in the supplementary materials.) The Raman spectra of samples C and F show a D line at 1338/cm of lower intensity than those for samples A and B, indicating fewer defects. However, the Raman spectrum of sample C shows a line of medium strength at 667/cm, which suggests the

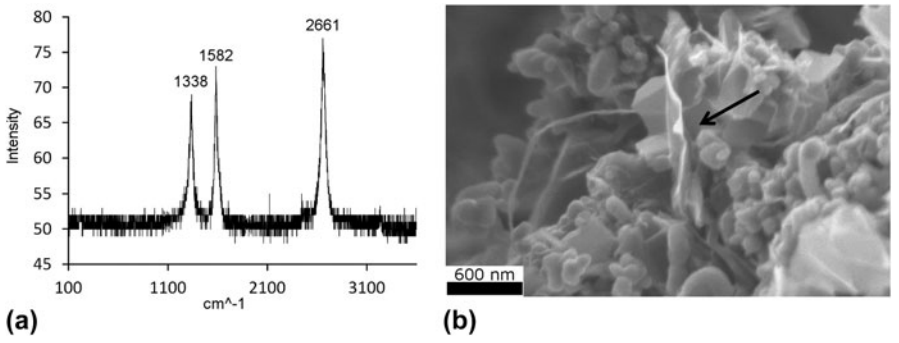


FIG. 1. (a) 632.8 nm laser excited Raman spectrum of sample A, the units in the abscissa are in 1/cm and the ordinate axis is the intensity in arbitrary units. (b) Typical SEM image of sample A, showing graphene sheets growing on catalyst particles. The edge of one such sheet is indicated by an arrow.

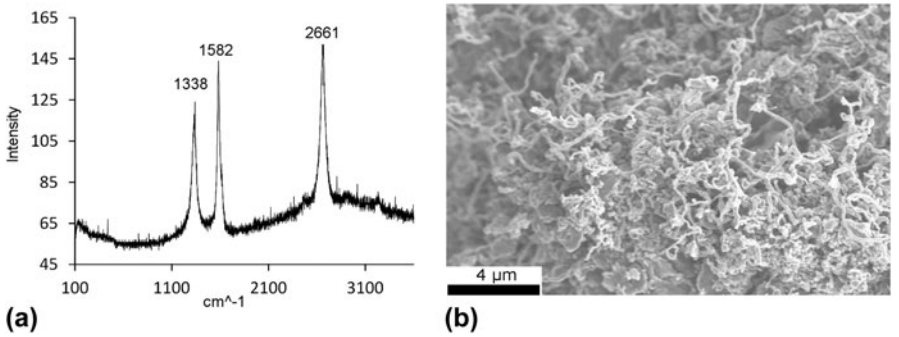


FIG. 2. (a) 632.8 nm laser excited Raman spectrum of sample B, the units in the abscissa are in 1/cm and the ordinate axis is the intensity in arbitrary units. (b) SEM image of sample B, showing a larger fraction of carbon nanotubes compared with sample A.

https://doi.org/10.1557/jmr.2014.165 Published online by Cambridge University Press

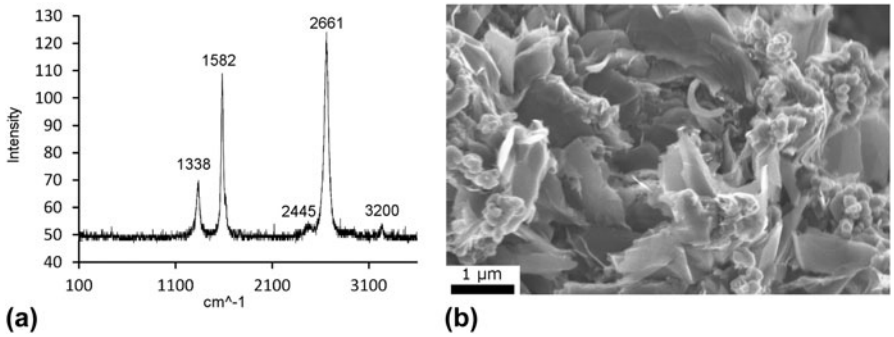


FIG. 3. (a) Raman spectra from sample F, the units in the abscissa are in 1/cm and the ordinate axis is the intensity in arbitrary units. (b) SEM image of sample F, displaying extensive growth of a large number of graphene sheets on the surface of the particles.

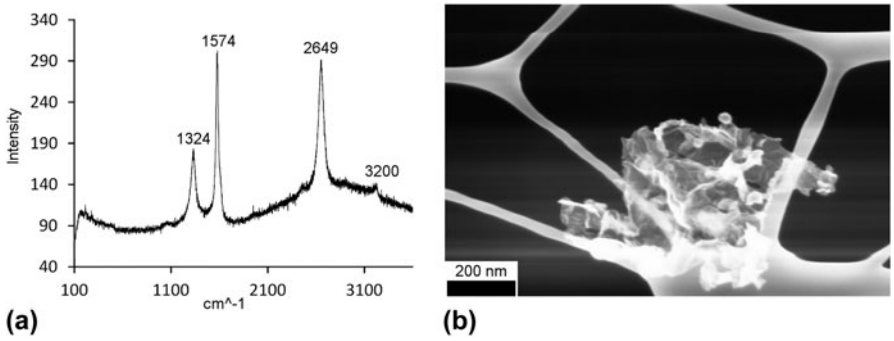


FIG. 4. (a) 632.8 nm laser excited Raman spectrum of acid purified sample G, the units in the abscissa are in 1/cm and the ordinate axis is the intensity in arbitrary units. (b) SEM image from sample G placed on a TEM grid.

formation of iron carbide. The Raman spectrum of sample F shows high quality, few layer graphene consistent with the SEM image in Fig. 3(b), which had a high concentration of graphene sheets. This sample was examined by TEM and the results are discussed below. The Raman spectrum of sample E, prepared without CO, still shows the formation of few layer graphene, hinting that the role of CO in graphene formation is not critical. Samples D and H do not show graphene growth based on the Raman data and SEM images. Intense Raman lines near 665/cm are likely to be associated with the formation of iron carbide, which would preclude the growth of graphene layers. This, in turn, would eliminate the G′ line, as observed in both samples. The absence of graphene and growth of iron carbide in samples D and H are likely to be due to the lack of acetylene (which decomposes to carbon at 800 °C) during the growth of sample D and sample H.

Sample F was purified with nitric acid to demonstrate that the metal can be removed, leaving pure graphene, which is sample G (Figs. 4 and 5). The Raman spectrum, however, shows some broadening of the G′ line and the appearance of a broad background due to disorder in the graphene structure. This indicates the purification process may cause some functionalization of the structure of graphene, while inducing disorder.

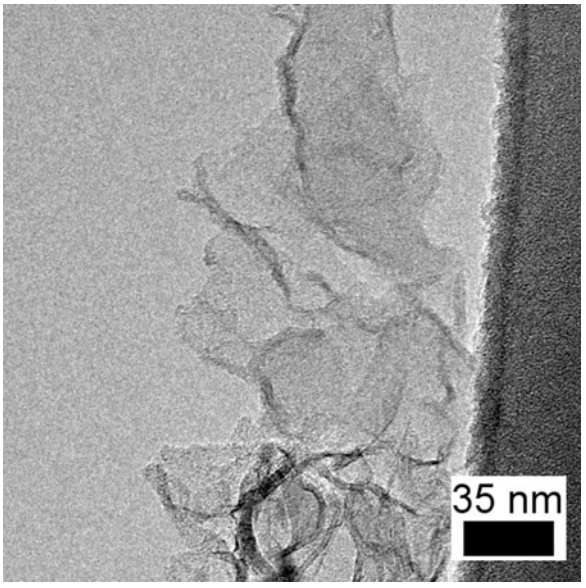


FIG. 5. TEM image of graphene with few layers forming a stack.

TEM was performed on sample F, which showed clear evidence for extensive growth of graphene. Note the presence of facets and folds in Fig. 6(a). Diffraction analysis shows that it is indeed few layer graphene, because the layer spacing is ≈3.4 Å and six-fold symmetry

https://doi.org/10.1557/jmr.2014.165 Published online by Cambridge University Press

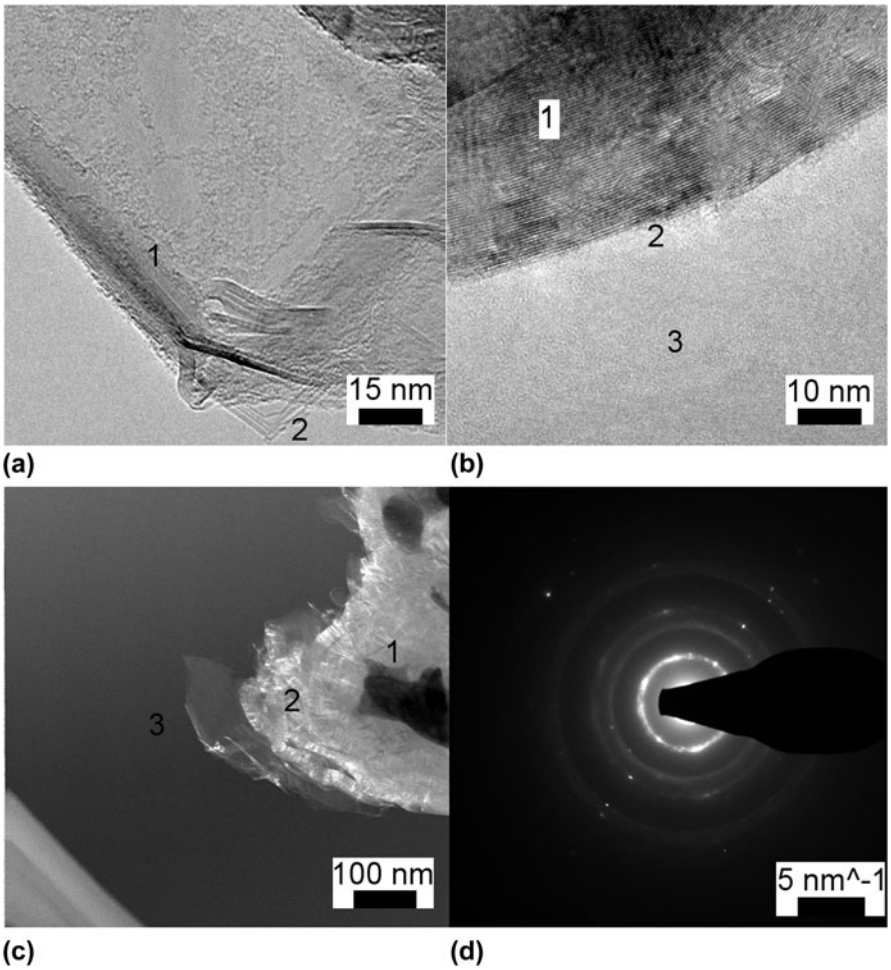


FIG. 6. (a) TEM image showing clear facets, which is an indication of the growth of graphene {[1]folds are evident, [2]right angles indicating faceted growth}. (b) TEM image showing the catalyst-iron interface. Whether there is an actual connection, or if the iron particle is simply on top of the graphene or vice versa, is unclear {[1]iron catalyst, [2]iron catalyst to graphene interface, [3]graphene}. (c) Scanning TEM image of the sample. Note the contrast can be used to find the iron catalyst and also examine the relative thickness of the graphene {[1]iron catalyst, [2]thick carbon, [3]graphene}. (d) Diffraction pattern showing 0.34 nm spacing and possible six-fold symmetry, indicative of layered carbon formation.

is evident. In Fig. 6(b), an image of the 'interface' between an iron catalyst and the graphene is given. The existence of the interface is critical for the determination of the growth mechanism of the graphene. Whether the graphene is actually bonded to the iron, or is just on top or below it is unclear from the image. A 'wall' model graphene sample would have a number of interfaces, while a flower model graphene sample would have very few if any (only forming after the initial growth of the graphene). A high degree of order is evident in the image, so atomic spacings can be resolved. Scanning TEM imaging was performed, combined with electron energy loss spectroscopy and energy dispersive x-ray analysis. This revealed that the darkest spots in the scanning TEM image were clusters of iron catalyst, which had carbon surrounding them. Toward the end of each of the layered carbon clusters, graphene sheets could be found. The catalyst is darkened in the image due to *Z* contrast. As one moves away from the catalyst, the growth of more single layers is evident. The carbon seems to surround clusters of iron particles, and after a critical point is reached, the layer opens up to form few layer or single layer graphene.

One possible mechanism of growth could be that several of the iron catalyst particles are simultaneously surrounded by carbon layers which fold out. This is opposed to VLS (vapor-liquid-solid) models of carbon nanotube growth, where carbon would layer around each individual catalyst particle. Since a large number of particles are surrounded by graphene, the layers are under tension and have a tendency of opening up, forming flat, graphitic plates. This favors the flower based model of growth discussed in the introduction. The wall method of growth seems unlikely, as one would expect the graphene which grew in that method to have dimensions restricted by the size of the catalyst particle. In the wall model, because they would only grow on one particle at a time,

https://doi.org/10.1557/jmr.2014.165 Published online by Cambridge University Press

at least one dimension of the sheet would be restricted to the circumference of the particle, which is approximately 63 nm on average for the 20 nm catalyst and 314 nm for the 100 nm catalyst, and this does not seem to be the case. Additional evidence for the flower model is the image in Fig. 6(c), which seems to be the material going through the 'bulb' phase into the 'flowering' phase. The folds found in various images, if real, further reinforce the flower model. The formation of graphene with folds in it would be more believable in a flower model than a wall model. Finally, the graphene infiltration failed to produce high strength composites. This would hint at the flower based model as the correct model. The interface, if real, found in Fig. 6(b) could be explained by the graphene forming initially through the flower model, and then diffusing into the iron later. A schematic depiction of the flower model is given in Fig. S3.

In conclusion, we have shown that few layer graphene can be grown using a relatively low temperature, scalable, and cost-effective CVD process and a commercially available catalyst nanopowder.

ACKNOWLEDGMENT

This work was supported by the US Army, ARDEC under contract W15QKN-10-D-0503-0002 and performed in the Iqbal group at the Chemistry and Environmental Science Department of the New Jersey Institute of Technology.[24] One of us (CY) was supported by Carbo-Met LLC.

REFERENCES

1. K.S. Novoselov, A.K. Geim, S.V. Morozov, D. Jiang, Y. Zhang, S.V. Dubonos, I.V. Grigorieva1, and A.A. Firsov: Electric field effect in atomically thin carbon films. *Science* **306**, 666 (2004).
2. Nobelprize.Org: *The Nobel Prize in Physics 2010*. [cited 31, Aug 2012]; Available from: http://www.nobelprize.org/nobel_prizes/physics/laureates/2010/ (2010).
3. A.K. Geim and K.S. Novoselov: The rise of graphene. *Nat. Mater.* **6**, 183 (2007).
4. Z. Chen, W. Ren, B. Liu, L. Gao, S. Pei, Z-S. Wu, J. Zhao, and H-M. Cheng: Bulk growth of mono- to few-layer graphene on nickel particles by chemical vapor deposition from methane. *Carbon* **48**, 3543 (2010).
5. M. Losurdo, M.M. Giangregorio, P. Capezzuto, and G. Bruno: Graphene CVD growth on copper and nickel: Role of hydrogen in kinetics and structure. *Phys. Chem. Chem. Phys.* **14**, 13 (2011).
6. A. Reina, S. Thiele, X. Jia, S. Bhaviripudi, M.S. Dresselhaus, J.A. Schaefer, and J. Kong: Growth of large-area single and Bi-layer graphene by controlled carbon precipitation on polycrystalline Ni surfaces. *Nano Res.* **2**, 509 (2009).
7. C. Mattevi, H. Kim, and M. Chhowalla: A review of chemical vapor deposition of graphene on copper. *J. Mater. Chem.* **21**, 3324 (2010).
8. K.S. Kim, Y. Zhao, H. Jang, S.Y. Lee, J.M. Kim, K.S. Kim, J-H. Ahn, P. Kim, J-Y. Choi, and B.H. Hong: Large-scale pattern growth of graphene films for stretchable transparent electrodes. *Nature* **457**, 706 (2008).
9. N.A. Vinogradov, A.A. Zakharov, V. Kocevski1, J. Rusz1, K.A. Simonov, O. Eriksson, A. Mikkelsen, E. Lundgren, A.S. Vinogradov, N. Mårtensson, and A.B. Preobrajenski: Formation and structure of graphene waves on Fe(110). *Phys. Rev. Lett.* **109**, 026101 (2012).
10. H. An, W-J. Lee, and J. Jung: Graphene synthesis on Fe foil using thermal CVD. *Curr. Appl. Phys.* **11**, S81 (2011).
11. A.S. Khan, Y.S. Suh, X. Chen, L. Takacs, and H. Zhang: Nanocrystalline aluminum and iron: Mechanical behavior at quasi-static and high strain rates, and constitutive modeling. *Int. J. Plast.* **22**, 195 (2006).
12. A. Goyal, D.A. Wiegand, F.J. Owens, and Z. Iqbal: Enhanced yield strength in iron nanocomposite with in situ grown single-wall carbon nanotubes. *J. Mater. Res.* **21**, 522 (2005).
13. A. Goyal, D.A. Wiegand, F.J. Owens, and Z. Iqbal: Synthesis of carbide-free, high strength iron-carbon nanotube composite by in situ nanotube growth. *Chem. Phys. Lett.* **442**, 365 (2007).
14. A. Goyal: New approaches to scaled-up carbon nanotube synthesis and nanotube-based metal composites and sensors. PhD Dissertation, New Jersey Institute of Technology, 2006.
15. R.B. Patel, J. Liu, S. Roy, S. Mitra, R.N. Dave, and Z. Iqbal: Formation of stainless steel–carbon nanotube composites using a scalable chemical vapor infiltration process. *J. Mater. Sci.* **48**, 1387 (2013).
16. R.B. Patel, J. Liu, J. Eng, and Z. Iqbal: One-step CVD synthesis of a boron nitride nanotube-iron composite. *J. Mater. Res.* **26**, 1332 (2011).
17. A.C. Ferrari, J.C. Meyer, V. Scardaci, C. Casiraghi, M. Lazzeri, F. Mauri, S. Piscanec, D. Jiang, K.S. Novoselov, S. Roth, and A. K. Geim: Raman spectrum of graphene and graphene layers. *Phys. Rev. Lett.* **97**, 187401 (2006).
18. A.C. Ferrari and D.M. Basko: Raman spectroscopy as a versatile tool for studying the properties of graphene. *Nat. Nanotechnol.* **8**, 235 (2013).
19. D. Graf, F. Molitor, K. Ensslin, C. Stampfer, A. Jungen, C. Hierold, and L. Wirtz: Spatially resolved Raman spectroscopy of single- and few-layer graphene. *Nano Lett.* **7**, 238–242 (2007).
20. C. Casiraghi, S. Pisana, K.S. Novoselov, A.K. Geim, and A.C. Ferrari: Raman fingerprint of charged impurities in graphene. *Appl. Phys. Lett.* **91**, 233108 (2007).
21. D.M. Basko: Theory of resonant multiphonon Raman scattering in graphene. *Phys. Rev. B* **78**, 125418 (2008).
22. L.M. Malard, M.A. Pimenta, G. Dresselhaus, and M.S. Dresselhaus: Raman spectroscopy in graphene. *Phys. Rep.* **473**, 51 (2009).
23. M.J. Matthews, M.A. Pimenta, G. Dresselhaus, M.S. Dresselhaus, and M. Endo: Origin of dispersive effects of the Raman D band in carbon materials. *Phys. Rev. B* **59**, R6585 (1999).
24. R.B. Patel: Synthesis and characterization of novel boron-based nanostructures and composites. PhD Dissertation, New Jersey Institute of Technology, 2013.

Supplementary Material

To view supplementary material for this article, please visit http://dx.doi.org/jmr.2014.165.

https://doi.org/10.1557/jmr.2014.165 Published online by Cambridge University Press